Brill Academic Publishers
P.O. Box 9000, 2300 PA Leiden,
The Netherlands

Lecture Series on Computer and Computational Sciences
Volume 1, 2006, pp. 1-10

Towards a black-box linear scaling optimization in Hartree-Fock and Kohn-Sham theories

Stinne Høst, Jeppe Olsen, Branislav Jansik, Poul Jørgensen[1]

Center for Theoretical Chemistry,
Department of Chemistry,
University of Aarhus,
DK-8000 Århus C, Denmark

Simen Reine, Trygve Helgaker

Department of Chemistry,
University of Oslo,
P. O. Box 1033 Blindern, N-0315 Norway

Paweł Sałek

Laboratory of Theoretical Chemistry,
The Royal Institute of Technology,
Teknikringen 30, Stockholm SE-10044, Sweden

Sonia Coriani

Dipartimento di Scienze Chimiche, Università degli Studi di Trieste, Via Licio Giorgieri 1,
I-34127 Trieste, Italy

Received 1 August, 2006; accepted in revised form ?? , 2006

Abstract: A linear scaling implementation of the trust-region self-consistent field (LS-TRSCF) method is described for the Hartree-Fock and Kohn-Sham calculations. The convergence of the method is examined and is in general smooth and robust and of equal quality for small and large systems. The LS-TRSCF calculations converge in several cases where conventional DIIS calculations diverge. The LS-TRSCF method may be recommended as the standard method for both small and large molecular systems.

Keywords: Linear scaling SCF, Hartree-Fock optimization, Kohn-Sham optimization, trust-region method

Mathematics Subject Classification: 31.15-p

1 Introduction

In Hartree-Fock (HF) and Kohn-Sham (KS) density functional theory (DFT), the electronic energy E_{SCF} is minimized with respect to the density of a single-determinantal wave function. In its original formulation, the minimization was carried out using the self-consistent field (SCF) method consisting of a sequence of Roothaan-Hall iterations. At each iteration, the Fock/KS matrix $\mathbf{F}$ is constructed from the current atomic-orbital (AO) density matrix $\mathbf{D}$; next, the Fock/KS matrix is diagonalized and finally an improved AO density matrix is determined from the molecular orbitals

[1]Corresponding author. E-mail: pou@chem.au.dk

(MOs) obtained by this diagonalization. Unfortunately, this simple SCF scheme converges only in simple cases.

To improve upon the convergence, the optimization is modified by constructing the Fock/KS matrix not directly from the AO density matrix of the last iteration, but rather from an averaged density matrix, obtained as a linear combination of the density matrices of the current and previous iterations. Typically, the averaged density matrix is obtained using the DIIS method of Pulay [1], by minimizing the norm of the corresponding linear combination of the gradients. The SCF/DIIS method has been implemented in most electronic-structure programs and has been successfully used to obtain optimized HF/KS energies. However, in some cases the DIIS procedure fails to converge.

During the last decade, much effort has been directed towards developing linear scaling SCF methods. In particular, the computational scaling for the evaluation of the Fock/KS matrix has been successfully reduced by use of the fast multipole method (FMM) for the Coulomb contribution [2]–[6], the order-N exchange (ONX) method and the linear exchange K (LinK) method for the exact (Hartree–Fock) exchange contribution [7]–[12], and efficient numerical quadrature methods for the exchange–correlation (XC) contribution [13]–[15]. Our SCF code uses FMM combined with density fitting for the Coulomb contribution, LinK for the exact exchange contribution, and linear-scaling numerical quadrature for the XC contribution. In the optimization of the SCF energy, the diagonalization of the Fock/KS matrix, which scales cubically with the system size (N^3), may therefore become the time dominating step for large molecules. In this paper, we discuss how the SCF method with DIIS may be improved upon by using an algorithm where the diagonalization of the Fock/KS matrix is avoided in favour of a method of linear complexity.

In the SCF/DIIS method, the minimization of the energy is carried out in two separate steps: the diagonalization of the Fock/KS matrix and the averaging of the density matrix. In neither step an energy lowering is enforced on E_{SCF}. It is simply hoped that, at the end of the SCF iterations, an optimized state is determined. We discuss improvements to both the diagonalization and the density matrix averaging, where a lowering of the energy E_{SCF} is enforced at each iteration. For both steps, we construct a local energy model to E_{SCF} with the current density matrix as the expansion point. At the expansion point, these models have the exact E_{SCF} gradient, but only an approximate Hessian. They are therefore valid only in a restricted region about the expansion point - the trust region. When these local models are used, it is essential that steps are only generated within the trust region, as otherwise no energy lowering is guaranteed.

Diagonalization is avoided by recognizing that the density matrix obtained by diagonalizing the Fock/KS matrix represents the global minimum of the Roothaan-Hall energy function $E^{\mathrm{RH}} = \mathrm{Tr}\,\mathbf{FD}$ (with fixed $\mathbf{F}$) [16]. The diagonalization may therefore be replaced by a minimization of E^{RH}. However, since E^{RH} is only a crude model of the true energy E_{SCF}, a complete minimization of E^{RH} (as obtained for example by diagonalization) may give steps that are too long to be trusted. When minimizing E^{RH}, we require the steps to be inside the trust region, solving a set of level shifted Newton equations where the level shift controls the size of the steps. The level shifted Newton equations may be solved using iterative algorithms where the time-dominating step is the multiplication of the Hessian by trialvectors. Linear complexity is therefore obtained by using sparse matrix algebra. The obtained algorithm will be denoted the linear scaling trust-region Roothaan-Hall (LS-TRRH) method.

To improve on the DIIS scheme we construct an energy function where the expansion coefficients of the averaged density matrix are the variational parameters. Carrying out a second-order expansion of this energy, using the quasi-Newton condition and neglecting terms that require evaluation of new Fock/KS matrices, we arrive at the density-subspace minimization (DSM) approximation to the energy E^{DSM} [17, 18]. At the expansion point, E^{DSM} has the same gradient as E_{SCF} and a good approximation to the Hessian. Again, trust-region optimization may be used to determine the optimal expansion coefficients, ensuring also an energy lowering at this step of the iteration

procedure. The obtained algorithm is denoted the trust-region density subspace minimization (TRDSM) method. Combining the LS-TRRH and TRDSM we obtain the LS-TRSCF method.

In the next section we describe the LS-TRRH algorithm while in section 3 the TRDSM algorithm is discussed. Section 4 contains numerical results which demonstrate the convergence of LS-TRSCF calculations and that linear scaling is obtained. The last section contains some concluding remarks.

2 Optimization of the Roothaan–Hall energy

2.1 Parametrization of the density matrix

Let $\mathbf{D}$ be a valid Kohn–Sham density matrix of an N-electron system, which together with the AO overlap matrix $\mathbf{S}$ satisfies the symmetry, trace and idempotency relations:

$$\mathbf{D}^{\mathrm{T}} = \mathbf{D} \tag{1}$$

$$\mathrm{Tr}\,\mathbf{DS} = N \tag{2}$$

$$\mathbf{DSD} = \mathbf{D} \tag{3}$$

Introducing the projectors $\mathbf{P}_{\mathrm{o}}$ and $\mathbf{P}_{\mathrm{v}}$ on the occupied and virtual spaces

$$\mathbf{P}_{\mathrm{o}} = \mathbf{DS} \tag{4}$$

$$\mathbf{P}_{\mathrm{v}} = \mathbf{I} - \mathbf{DS} \tag{5}$$

we may, from the reference density matrix $\mathbf{D}$, generate any other valid density matrix by the transformation [16, 20, 21]

$$\mathbf{D}(\mathbf{X}) = \exp\left[-\mathcal{P}(\mathbf{X})\mathbf{S}\right]\mathbf{D}\exp\left[\mathbf{S}\mathcal{P}(\mathbf{X})\right] \tag{6}$$

where $\mathbf{X}$ is an anti-Hermitian matrix and where

$$\mathcal{P}(\mathbf{X}) = \mathbf{P}_{\mathrm{o}}\mathbf{X}\mathbf{P}_{\mathrm{v}}^{\mathrm{T}} + \mathbf{P}_{\mathrm{v}}\mathbf{X}\mathbf{P}_{\mathrm{o}}^{\mathrm{T}} \tag{7}$$

project out the redundant occupied-occupied and virtual-virtual components of $\mathbf{X}$.

The density-matrix $\mathbf{D}(\mathbf{X})$ may be expanded in orders of $\mathbf{X}$ as

$$\mathbf{D}(\mathbf{X}) = \mathbf{D} + \left[\mathbf{D}, \mathcal{P}(\mathbf{X})\right]_{\mathrm{S}} + \tfrac{1}{2}\left[\left[\mathbf{D}, \mathcal{P}(\mathbf{X})\right]_{\mathrm{S}}, \mathcal{P}(\mathbf{X})\right]_{\mathrm{S}} + \cdots \tag{8}$$

where we have introduced the S commutator

$$\left[\mathbf{A}, \mathbf{B}\right]_{\mathrm{S}} = \mathbf{ASB} - \mathbf{BSA} \tag{9}$$

2.2 The Roothaan–Hall Newton equations in the AO basis

In an SCF optimization, the diagonalization of the Fock/KS matrix $\mathbf{F}$ is equivalent to the minimization of the Roothaan–Hall energy [16]

$$E^{\mathrm{RH}}(\mathbf{X}) = \mathrm{Tr}\left[\mathbf{FD}(\mathbf{X})\right] \tag{10}$$

in the sense that both approaches yield the same density matrix. Inserting the S-commutator expansion of the density matrix $\mathbf{D}(\mathbf{X})$, we obtain

$$\begin{aligned}\mathrm{Tr}\left[\mathbf{FD}(\mathbf{X})\right] = \mathrm{Tr}\left(\mathbf{FD}\right) &+ \mathrm{Tr}\left(\mathbf{F}^{\mathrm{vo}}\mathbf{X} - \mathbf{M}^{\mathrm{ov}}\mathbf{X}\right) \\ &+ \mathrm{Tr}\left(\mathbf{F}^{\mathrm{oo}}\mathbf{X}\mathbf{S}^{\mathrm{vv}}\mathbf{X} - \mathbf{F}^{\mathrm{vv}}\mathbf{X}\mathbf{S}^{\mathrm{oo}}\mathbf{X}\right) + \cdots\end{aligned} \tag{11}$$

where we have made repeated use of the idempotency relations $\mathbf{P}_{\mathrm{o}}^2 = \mathbf{P}_{\mathrm{o}}$ and $\mathbf{P}_{\mathrm{v}}^2 = \mathbf{P}_{\mathrm{v}}$ and of the orthogonality relations $\mathbf{P}_{\mathrm{o}}\mathbf{P}_{\mathrm{v}} = \mathbf{P}_{\mathrm{v}}\mathbf{P}_{\mathrm{o}} = \mathbf{0}$ and $\mathbf{P}_{\mathrm{o}}^{\mathrm{T}}\mathbf{S}\mathbf{P}_{\mathrm{v}} = \mathbf{P}_{\mathrm{v}}^{\mathrm{T}}\mathbf{S}\mathbf{P}_{\mathrm{o}} = \mathbf{0}$ and introduced the short-hand notation

$$\mathbf{F}^{\mathrm{ab}} = \mathbf{P}_{\mathrm{a}}^{\mathrm{T}}\mathbf{F}\mathbf{P}_{\mathrm{b}} \tag{12}$$

Note that, whereas the off-diagonal projections $\mathbf{F}^{\mathrm{ov}}$ and $\mathbf{F}^{\mathrm{vo}}$ of $\mathbf{F}$ contribute to the terms linear in $\mathbf{X}$, the diagonal projections $\mathbf{F}^{\mathrm{oo}}$ and $\mathbf{F}^{\mathrm{vv}}$ contribute to the quadratic terms.

The Roothaan-Hall energy E^{RH} is only a crude model of the true HF/KS energy E_{SCF}, having the correct gradient but an approximate Hessian at the point of expansion; this can be understood from the observation that, whereas E^{RH} depends linearly on $\mathbf{D}(\mathbf{X})$, the true energy E_{SCF} depends quadratically on $\mathbf{D}(\mathbf{X})$. Therefore, a complete minimization of E^{RH} (as achieved, for example, by diagonalization of the Fock/KS matrix), may give steps that are too long to be trusted. Such steps may, for example, increase rather than decrease the total SCF energy. We therefore impose on the energy minimization the constraint that the new occupied space does not differ appreciably from the old occupied space. The step must therefore be inside or on the boundary of the trust region of E^{RH}, which we define as a hypersphere with radius h around the density at the current expansion point. In the $\mathbf{S}$ metric norm, the length of the step

$$||\mathcal{P}(\mathbf{X})||_S^2 = \mathrm{Tr}[\mathcal{P}(\mathbf{X})\mathbf{S}\mathcal{P}(\mathbf{X})\mathbf{S}] \tag{13}$$

is thus restricted to h^2. To satisfy this constraint, we introduce an undetermined multiplier μ and set up the Lagrangian

$$L^{\mathrm{RH}}(\mathbf{X}) = \mathrm{Tr}\left[\mathbf{F}\mathbf{D}(\mathbf{X})\right] - \frac{1}{2}\mu\left(\mathrm{Tr}[\mathcal{P}(\mathbf{X})\mathbf{S}\mathbf{X}\mathbf{S}] - h^2\right) \tag{14}$$

Expanding this Lagrangian to second order in $\mathbf{X}$ using Eq. (11), we obtain

$$\begin{aligned} L^{\mathrm{RH}}(\mathbf{X}) = {} & \mathrm{Tr}\left(\mathbf{F}\mathbf{D}\right) + \mathrm{Tr}\left(\mathbf{F}^{\mathrm{vo}}\mathbf{X} - \mathbf{F}^{\mathrm{ov}}\mathbf{X}\right) \\ & + \mathrm{Tr}\left(\mathbf{F}^{\mathrm{oo}}\mathbf{X}\mathbf{S}^{\mathrm{vv}}\mathbf{X} - \mathbf{F}^{\mathrm{vv}}\mathbf{X}\mathbf{S}^{\mathrm{oo}}\mathbf{X}\right) + \mu\left[\mathrm{Tr}\left(\mathbf{S}^{\mathrm{oo}}\mathbf{X}\mathbf{S}^{\mathrm{vv}}\mathbf{X}\right) - \frac{1}{2}h^2\right]\cdots \end{aligned} \tag{15}$$

Differentiating this function with respect to the elements of $\mathbf{X}$, we obtain

$$\begin{aligned} \frac{\partial L^{\mathrm{RH}}(\mathbf{X})}{\partial \mathbf{X}} = {} & \mathbf{F}^{\mathrm{ov}} - \mathbf{F}^{\mathrm{vo}} - \mathbf{S}^{\mathrm{vv}}\mathbf{X}\mathbf{F}^{\mathrm{oo}} - \mathbf{F}^{\mathrm{oo}}\mathbf{X}\mathbf{S}^{\mathrm{vv}} + \mathbf{F}^{\mathrm{vv}}\mathbf{X}\mathbf{S}^{\mathrm{oo}} + \mathbf{S}^{\mathrm{oo}}\mathbf{X}\mathbf{F}^{\mathrm{vv}} \\ & - \mu\left(\mathbf{S}^{\mathrm{vv}}\mathbf{X}\mathbf{S}^{\mathrm{oo}} + \mathbf{S}^{\mathrm{oo}}\mathbf{X}\mathbf{S}^{\mathrm{vv}}\right) + \cdots \end{aligned} \tag{16}$$

where we have used the relation

$$\frac{\partial\,\mathrm{Tr}(\mathbf{A}\mathbf{X})}{\partial \mathbf{X}} = \mathbf{A}^{\mathrm{T}} \tag{17}$$

Finally, setting the right-hand side equal to zero and ignoring higher-order contributions, we obtain the matrix equation

$$\begin{aligned} & \mathbf{F}^{\mathrm{vv}}\mathbf{X}\mathbf{S}^{\mathrm{oo}} - \mathbf{F}^{\mathrm{oo}}\mathbf{X}\mathbf{S}^{\mathrm{vv}} + \mathbf{S}^{\mathrm{oo}}\mathbf{X}\mathbf{F}^{\mathrm{vv}} - \mathbf{S}^{\mathrm{vv}}\mathbf{X}\mathbf{F}^{\mathrm{oo}} \\ & \qquad - \mu\left(\mathbf{S}^{\mathrm{vv}}\mathbf{X}\mathbf{S}^{\mathrm{oo}} + \mathbf{S}^{\mathrm{oo}}\mathbf{X}\mathbf{S}^{\mathrm{vv}}\right) = \mathbf{F}^{\mathrm{vo}} - \mathbf{F}^{\mathrm{ov}} \end{aligned} \tag{18}$$

for the stationary points on the trust sphere of the Roothaan–Hall energy function.

Eq. (18) is equivalent to a level shifted sef of Newton equations

$$(\mathbf{H} - \mu\mathbf{M})\mathbf{x} = \mathbf{G} \tag{19}$$

where

$$\mathbf{H} = \mathbf{F}^{\mathrm{vv}} \otimes \mathbf{S}^{\mathrm{oo}} - \mathbf{F}^{\mathrm{oo}} \otimes \mathbf{S}^{\mathrm{vv}} + \mathbf{S}^{\mathrm{oo}} \otimes \mathbf{F}^{\mathrm{vv}} - \mathbf{S}^{\mathrm{vv}} \otimes \mathbf{F}^{\mathrm{oo}} \tag{20}$$

$$\mathbf{M} = \mathbf{S}^{\mathrm{vv}} \otimes \mathbf{S}^{\mathrm{oo}} - \mathbf{S}^{\mathrm{oo}} \otimes \mathbf{S}^{\mathrm{vv}} \tag{21}$$

$$\mathbf{G} = \mathrm{Vec}(\mathbf{F}^{\mathrm{vo}} - \mathbf{F}^{\mathrm{ov}}) \tag{22}$$

$$\mathbf{x} = \mathrm{Vec}\mathbf{X} \tag{23}$$

2.3 The Roothaan–Hall Newton equations in an orthonormal basis

The conditioning number of the level shifted Hessian matrix in Eq. (19) is greatly reduced by transforming the equation to an orthogonal basis. We consider transformations based on the factorization of the overlap in the form

$$\mathbf{S} = \mathbf{V}^{\mathrm{T}}\mathbf{V} \tag{24}$$

Such a factorization may be accomplished in infinitely many ways – for example, by introducing a Cholesky factorization (as employed by Shao *et al.* [22] in the curvy step method) or the principal square root

$$\mathbf{V}_{\mathrm{c}} = \mathbf{U} \tag{25}$$

$$\mathbf{V}_{\mathrm{s}} = \mathbf{S}^{1/2} \tag{26}$$

where $\mathbf{U}$ is an nonsingular upper triangular matrix and where $\mathbf{S}^{1/2}$ is a positive-definite symmetric matrix. In the orthonormal basis, the Roothaan–Hall Newton equations Eq. (18) take the form

$$(\mathbf{F}_{\mathrm{V}}^{\mathrm{vv}} - \mathbf{F}_{\mathrm{V}}^{\mathrm{oo}} - \mu\mathbf{I})\mathbf{X}^{\mathrm{V}} + \mathbf{X}^{\mathrm{V}}(\mathbf{F}_{\mathrm{V}}^{\mathrm{vv}} - \mathbf{F}_{\mathrm{V}}^{\mathrm{oo}} - \mu\mathbf{I}) = \mathbf{F}_{\mathrm{V}}^{\mathrm{vo}} - \mathbf{F}_{\mathrm{V}}^{\mathrm{ov}} \tag{27}$$

where we have introduced the notation

$$\mathbf{A}_{\mathrm{V}} = \mathbf{V}^{-\mathrm{T}}\mathbf{A}\mathbf{V}^{-1} \tag{28}$$

$$\mathbf{A}^{\mathrm{V}} = \mathbf{V}\mathbf{A}\mathbf{V}^{\mathrm{T}} \tag{29}$$

and where we have further assumed that $\mathbf{X}^{\mathrm{V}}$ contains only non-redundant components. When solving Eq. (27) by the conjugate gradient method, it is advantageous to use a diagonal preconditioner.

Eq. (27) represents the solution of a level shifted Newton set of linear equations

$$\mathbf{H}_{\mathrm{V}}\mathbf{x}^{\mathrm{V}} - \mu\mathbf{I}\mathbf{x}^{\mathrm{V}} = \mathbf{G}_{\mathrm{V}} \tag{30}$$

where

$$\mathbf{H}_{\mathrm{V}} = (\mathbf{F}_{\mathrm{V}}^{\mathrm{vv}} - \mathbf{F}_{\mathrm{V}}^{\mathrm{oo}}) \otimes \mathbf{I} + \mathbf{I} \otimes (\mathbf{F}_{\mathrm{V}}^{\mathrm{vv}} - \mathbf{F}_{\mathrm{V}}^{\mathrm{oo}}) \tag{31}$$

$$\mathbf{x}^{\mathrm{V}} = \mathrm{Vec}\mathbf{X}^{\mathrm{V}} \tag{32}$$

$$\mathbf{G}_{\mathrm{V}} = \mathrm{Vec}(\mathbf{F}_{\mathrm{V}}^{\mathrm{vo}} - \mathbf{F}_{\mathrm{V}}^{\mathrm{ov}}) \tag{33}$$

In the global region of an SCF optimization, the boundary of the trust region is represented by $X_{\mathrm{V}}^{\max} = k$, where $X_{\mathrm{V}}^{\max}$ is the largest component of $\mathbf{X}^{\mathrm{V}}$ and k is 0.35. Unlike $||\mathbf{X}^{\mathrm{V}}||_S$, $X_{\mathrm{V}}^{\max}$ is size-extensive, provided equal diagonal dominance of the Hessian matrix for small and large systems.

To ensure that the minimum is determined on the boundary of the trust region, the level shift must be restricted to the interval $-\infty < \mu < \epsilon_{\min}$ where $\epsilon_{\min}$ is the lowest eigenvalue of the Hessian Eq. (31). In principle, the lowest Hessian eigenvalue should therefore be determined and

a line search carried out in the interval $-\infty < \mu < \epsilon_{\min}$ to find the level shift μ with $X_{\mathrm{V}}^{\max} = 0.35$. However, a simpler strategy is obtained by recognizing that the solution of the level shifted Newton equations can be determined from the eigenvectors of the augmented Hessian eigenvalue equation [23, 24, 25]. If the solution with the lowest eigenvalue is determined, the level shift is restricted to the interval $-\infty < \mu < \epsilon_{\min}$.

The level shifted Newton equations may be solved using an iterative procedure where the reduced space Hessians and gradients are set up in each iteration. At each iteration, the augmented Hessian may therefore also be set up at essentially no cost and the lowest eigenvalue determined. Consequently the level shift may be updated by solving the reduced space augmented Hessian eigenvalue problem at no extra cost. With the updated level shift, a new Newton iteration may be carried out and the iterations continued until convergence is obtained with respect to level shift and the residual of the Newton equations (see Ref. [26]).

When the level shifted Newton equations are solved using iterative algorithms, the time consuming step is the linear transformation of the Hessian matrix on trial vectors. Using sparse matrix algebra, linear scaling may be obtained in these linear transformations.

3 The density-subspace minimization (DSM) algorithm

After a sequence of Roothaan–Hall iterations, we have determined a set of density matrices $\mathbf{D}_i$ and a corresponding set of Fock/KS matrices $\mathbf{F}_i = \mathbf{F}(\mathbf{D}_i)$. We now discuss how to make the best use of the information contained in these matrices.

3.1 Parametrization of the DSM density matrix

Using $\mathbf{D}_0$ as the reference density matrix, the improved density matrix may be expressed as a linear combination of the current and previous density matrices [17, 18]

$$\overline{\mathbf{D}} = \mathbf{D}_0 + \sum_{i=0}^{n} c_i \mathbf{D}_i. \tag{34}$$

Ideally $\overline{\mathbf{D}}$ should satisfy the symmetry, trace and idempotency conditions Eqs. (1-3). The symmetry condition Eq. (1) is trivially satisfied while the trace condition Eq. (2) holds only if

$$c_0 = -\sum_{i=1}^{n} c_i. \tag{35}$$

Using c_i with $1 \leq i \leq n$ as independent parameters the density matrix $\overline{\mathbf{D}}$ may be expressed as

$$\overline{\mathbf{D}} = \mathbf{D}_0 + \mathbf{D}_+, \tag{36}$$

where we have introduced the notation

$$\mathbf{D}_+ = \sum_{i=1}^{n} c_i \mathbf{D}_{i0}, \tag{37a}$$

$$\mathbf{D}_{i0} = \mathbf{D}_i - \mathbf{D}_0. \tag{37b}$$

While $\overline{\mathbf{D}}$ satisfies the symmetry and trace conditions Eqs. (1) and (2), the idempotency condition Eq. (3) is not fulfilled. A smaller idempotency error may be obtained using the purified density matrix of McWeeny [19, 27]

$$\widetilde{\mathbf{D}} = 3\overline{\mathbf{D}}\mathbf{S}\overline{\mathbf{D}} - 2\overline{\mathbf{D}}\mathbf{S}\overline{\mathbf{D}}\mathbf{S}\overline{\mathbf{D}}. \tag{38}$$

Emphasizing that $\mathbf{D}_0$ is the reference density matrix, the first-order purified density matrix may be expressed as

$$\widetilde{\mathbf{D}} = \mathbf{D}_0 + \mathbf{D}_+ + \mathbf{D}_\delta. \tag{39}$$

where we have introduced the idempotency correction

$$\mathbf{D}_\delta = \widetilde{\mathbf{D}} - \overline{\mathbf{D}}. \tag{40}$$

3.2 Construction of the DSM energy function

Expanding the energy for the purified averaged density matrix, Eq. (39), around the reference density matrix $\mathbf{D}_0$, we obtain to second order

$$E(\widetilde{\mathbf{D}}) = E(\mathbf{D}_0) + (\mathbf{D}_+ + \mathbf{D}_\delta)^{\mathrm{T}}\, \mathbf{E}_0^{(1)} + \frac{1}{2}\,(\mathbf{D}_+ + \mathbf{D}_\delta)^{\mathrm{T}}\, \mathbf{E}_0^{(2)}\,(\mathbf{D}_+ + \mathbf{D}_\delta) \tag{41}$$

To evaluate the terms containing $\mathbf{E}_0^{(1)}$ and $\mathbf{E}_0^{(2)}$, we first recall that the Fock/KS matrix is defined as

$$\mathbf{E}_0^{(1)} = 2\mathbf{F}_0 \tag{42}$$

Next we carry out an expansion of $\mathbf{E}_i^{(1)}$ with $\mathbf{D}_0$ as expansion point

$$\mathbf{E}_i^{(1)} = \mathbf{E}_0^{(1)} + \mathbf{E}_0^{(2)}(\mathbf{D}_i - \mathbf{D}_0) + \mathcal{O}\big(\mathbf{D}_i - \mathbf{D}_0\big)^2 \tag{43}$$

Neglecting terms of order $\mathcal{O}\big(\mathbf{D}_i - \mathbf{D}_0\big)^2$ we obtain the quasi–Newton condition

$$\mathbf{E}_0^{(2)}(\mathbf{D}_i - \mathbf{D}_0) = 2\mathbf{F}_i - 2\mathbf{F}_0 = 2\mathbf{F}_{i0} \tag{44}$$

which may be used to obtain

$$\mathbf{E}_0^{(2)}\mathbf{D}_+ = 2\mathbf{F}_+ + \mathcal{O}(\mathbf{D}_+^2), \tag{45}$$

where we have generalized the notation Eq. (37a) to the Fock/KS matrix

$$\mathbf{F}_+ = \sum_{i=1}^{n} c_i \mathbf{F}_{i0} \tag{46}$$

Using Eq. (42) and Eq. (45) and ignoring the terms quadratic in $\mathbf{D}_\delta$ in Eq. (41) and quadratic in $\mathbf{D}_+$ in Eq. (45), we then obtain the DSM energy

$$E^{\mathrm{DSM}}(\mathbf{c}) = E(\mathbf{D}_0) + 2\,\mathrm{Tr}\,\mathbf{D}_+\mathbf{F}_0 + \mathrm{Tr}\,\mathbf{D}_+\mathbf{F}_+ + 2\,\mathrm{Tr}\,\mathbf{D}_\delta\mathbf{F}_0 + 2\,\mathrm{Tr}\,\mathbf{D}_\delta\mathbf{F}_+. \tag{47}$$

Note that $E^{\mathrm{DSM}}(\mathbf{c})$ is expressed solely in terms of the density and Fock/KS matrices of the current and previous iterations. For a more compact notation, we introduce the weighted Fock/KS matrix

$$\overline{\mathbf{F}} = \mathbf{F}_0 + \mathbf{F}_+ = \mathbf{F}_0 + \sum_{i=1}^{n} c_i \mathbf{F}_{i0} \tag{48}$$

and find that the DSM energy may be written in the form

$$E^{\mathrm{DSM}}(\mathbf{c}) = E(\overline{\mathbf{D}}) + 2\,\mathrm{Tr}\,\mathbf{D}_\delta\overline{\mathbf{F}}, \tag{49}$$

where the first term is quadratic in the expansion coefficients c_i

$$E(\overline{\mathbf{D}}) = E(\mathbf{D}_0) + 2\,\mathrm{Tr}\,\mathbf{D}_+\mathbf{F}_0 + \mathrm{Tr}\,\mathbf{D}_+\mathbf{F}_+, \tag{50}$$

and the second (idempotency correction) term is quartic in these coefficients:

$$2\,\mathrm{Tr}\,\mathbf{D}_\delta\overline{\mathbf{F}} = \mathrm{Tr}(6\overline{\mathbf{D}}\mathbf{S}\overline{\mathbf{D}} - 4\overline{\mathbf{D}}\mathbf{S}\overline{\mathbf{D}}\mathbf{S}\overline{\mathbf{D}} - 2\overline{\mathbf{D}})\overline{\mathbf{F}}. \tag{51}$$

The derivatives of $E^{\mathrm{DSM}}(\mathbf{c})$ are straightforwardly obtained by inserting the expansions of $\overline{\mathbf{F}}$ and $\overline{\mathbf{D}}$, using the independent parameter representation and the minimization of $E^{\mathrm{DSM}}(\mathbf{c})$ may straightforwardly be carried out using the trust-region method.

4 Numerical Illustrations

4.1 Convergence of test calculations

We now describe the convergence of test calculations for Hartree-Fock and DFT LDA using the LS-TRSCF algorithm where the level shifted Newton equations are solved in the basis defined by the principal square root in Eq. (26). For comparison, the convergence of the standard SCF/DIIS calculations (diagonalization + DIIS, no level shift) will also be reported. In both DIIS and TRDSM a maximum of eight densities and Fock/KS matrices stored.

In Fig. 1 we display the convergence (the difference between the energy of a given iteration and the converged energy) of Hartree-Fock calculations using LS-TRSCF (left panel) and SCF/DIIS (right panel) on six molecules representing different types of chemical compounds: 1). Water, stretched: H_2O where the O−H bond is twice its equilibrium value (d-aug-pVTZ basis). 2). Zn complex: The zinc-EDDS complex of Ref. [18] (6-31G basis). 3). Rh complex: The rhodium complex of Ref. [17] (AhlrichsVDZ basis [28], STO-3G on Rh). 4). Cd complex: The cadmium-imidazole complex of Ref. [18] (3-21G basis). 5). Polysaccharide: A polysaccharide containing 438 atoms (6-31G basis). 6). Polyalanine, 24 units: A polypeptide containing 24 alanine residues (6-31G basis). Smooth convergence to 10^{-8} a.u. is obtained in all LS-TRSCF calculations. Convergence is obtained in between 12-30 iterations. The convergence is very similar for the SCF/DIIS and the LS-TRSCF calculations except for the rhodium complex, where the SCF/DIIS calculation diverges while smooth convergence is obtained using the TRSCF algorithm. The local convergence is very similar for SCF/DIIS and LS-TRSCF reflecting that in both DIIS and DSM, the local convergence is determined by the fact that the quasi Newton condition is satisfied [18]. In Fig. 2, we report calculations similar to those in Fig. 1 but where the Hartree-Fock model is replaced by LDA. The convergence of the LS-TRSCF Hartree-Fock and LDA calculations is very similar with the exception of the Rh complex where the LDA calculation has a rather erratic behaviour from about iteration 20 to 80 after which fast convergence is obtained. The SCF/DIIS LDA calculations in the left panel in Fig. 2 show erratic convergence behaviour in particular for the Cd complex and polyalanine where the calculations diverge, and for the polysaccharide calculation in the initial 25 iterations. The erratic behaviour which is in general observed in the initial iterations of SCF/DIIS calculations reflects that energy lowering is not an agenda in the SCF/DIIS scheme. Surprisingly, the SCF/DIIS LDA calculation on the rhodium complex converges, while the corresponding Hartree-Fock calculation diverges. To sum it up, similar convergence is seen in Hartree-Fock SCF/DIIS and the LS-TRSCF calculations, whereas for LDA, a much more smooth and robust convergence is obtained by using the LS-TRSCF scheme. Particularly in the initial iterations, a more erratic behaviour is seen with the SCF/DIIS algorithm. In several cases LS-TRSCF calculations converge, where SCF/DIIS calculations diverge.

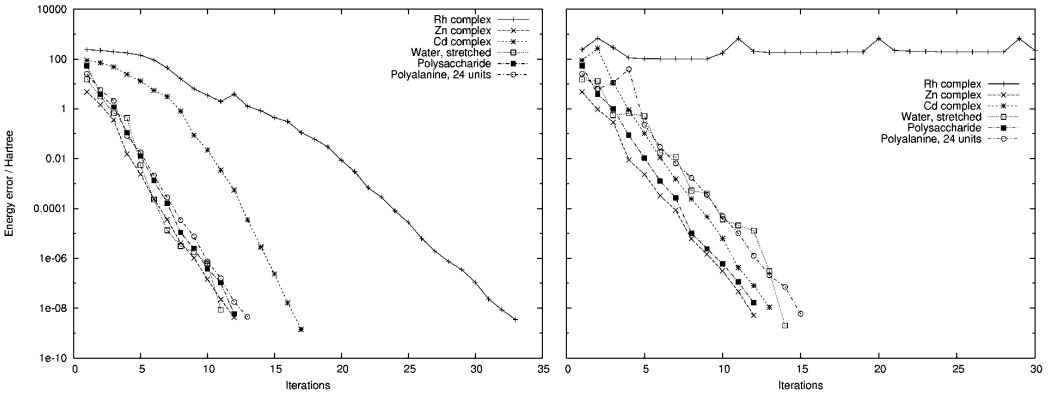

Figure 1: Convergence of the Hartree-Fock LS-TRSCF (left panel) and SCF/DIIS (right panel) calculations for the rhodium complex, the zinc complex, the cadmium complex, the stretched water, the polysaccharide and the polyalanine. The energy error (a.u.) in each iteration is plotted versus number of iterations.

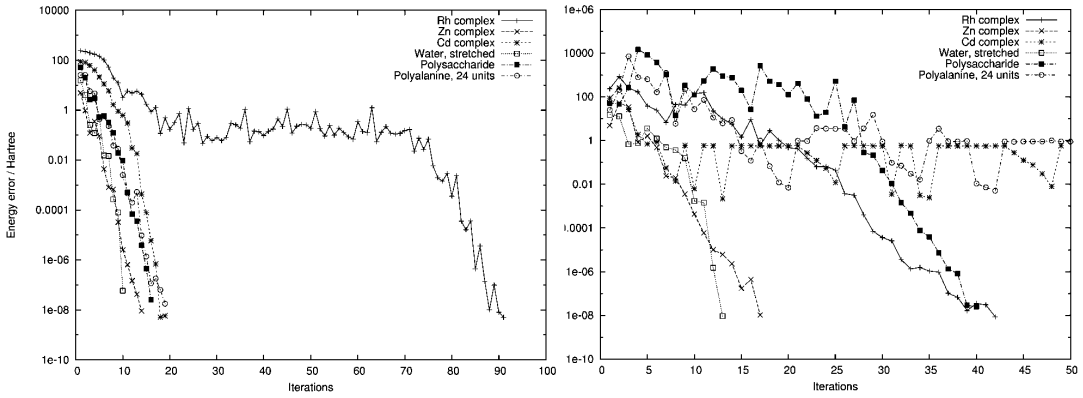

Figure 2: Convergence of the LDA LS-TRSCF (left panel) and SCF/DIIS (right panel) calculations for the rhodium complex, the zinc complex, the cadmium complex, the stretched water, the polysaccharide and the polyalanine. The energy error (a.u.) in each iteration is plotted versus number of iterations.

4.2 Linear scaling using the LS-TRSCF algorithm

In this subsection, we will illustrate that linear scaling is obtained using the LS-TRSCF algorithm. We consider calculations on a polyalanine chain where we extend the number of alanine residues. We consider both Hartree-Fock and B3LYP calculations in a 6-31G basis. The largest alanine chain contains 119 alanine residues (a total of 1192 atoms). The convergence of an alanine calculation with 24 alanine units is given in Figs. 1-2.

In Fig. 3 we have shown the CPU time used in the different parts of the LS-TRSCF algorithm for the Hartree-Fock calculations using the sparse matrix representation. In all figures, the timings are for the first iteration in the local region, except for the DSM time, which is dependent on the number of previous densities. Therefore, the DSM time is always given for iteration 8, where we have the maximum number of previous densities involved. The timings are given for the evaluation of the Coulomb (Fock J) and exchange (Fock X) parts of the Fock/KS matrix, respectively, and for the LS-TRRH step and for the TRDSM step. The curve for the most expensive step – the exchange part of the Fock matrix – has a bend due to an N^2 scaling sorting routine. For both the LS-TRRH and TRDSM steps, the time consuming part of the calculations consists mainly of matrix multiplications. Both LS-TRRH and TRDSM scale linearly with system size in the calculations in Fig. 3, where sparsity is exploited in the matrix multiplications. The benefits from

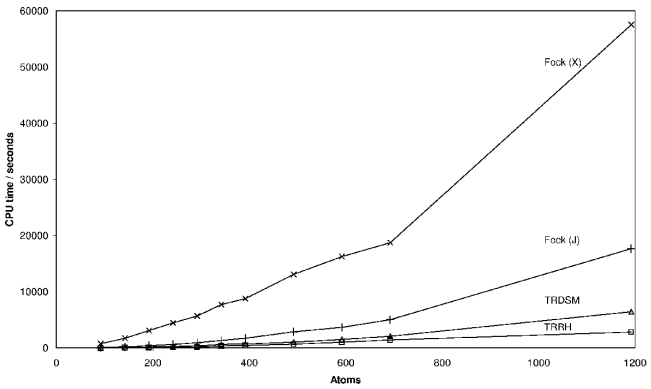

Figure 3: CPU timings for one iteration of a Hartree-Fock calculation using a 6-31G basis plotted as a function of the number of atoms in a polyalanine peptide. The considered contributions are the exchange (X) and Coulomb (J) contributions to Fock matrix in addition to the LS-TRRH and TRDSM optimization steps where sparse matrix algebra is used.

exploiting the sparsity of the involved matrices become evident from Fig. 4, where we have plotted the CPU times for the LS-TRRH and TRDSM steps from Fig. 3 in combination with timings for calculations where the matrix multiplications involve full (dense) matrices. The timings for full matrix representations increase with system size in accorcance with cubic scaling, but become linear when the sparsity is exploited. As seen on the figure, the advantage of going to the sparse matrix representation has an earlier onset for TRDSM than for LS-TRRH, because TRDSM contains more matrix multiplications than LS-TRRH. Fig. 5 shows the CPU timings for the B3LYP calculations in the sparse matrix representation. The timings shown are the same as in Fig. 3, with the addition of the timing for the exchange-correlation (Kohn-Sham XC) contribution. Like the other contributions to the KS matrix (Coulomb and exchange), the exchange-correlation contribution has reached the linear scaling regime. In general, the behaviour of the B3LYP curves is similar to the one observed for the HF curves.

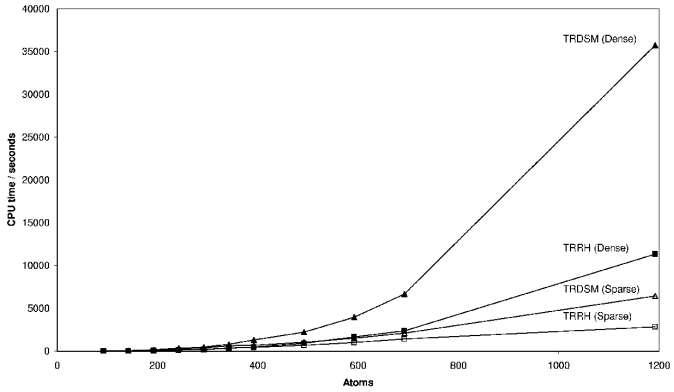

Figure 4: CPU timings for one iteration of a Hartree-Fock calculation using a 6-31G basis for the LS-TRRH and TRDSM steps for sparse and dense matrices plotted as a function of the number of atoms in a polyalanine peptide.

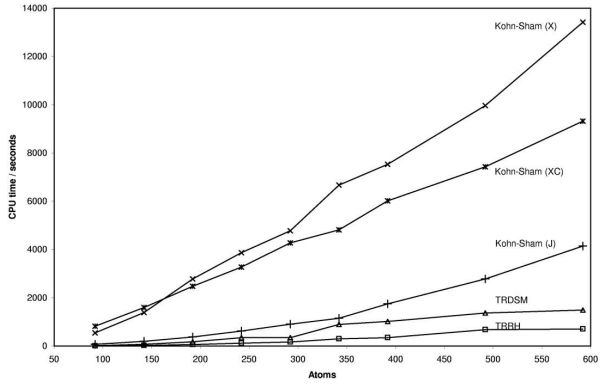

Figure 5: CPU timings for one iteration of a B3LYP calculation using a 6-31G basis plotted as a function of the number of atoms in a polyalanine peptide. The same contributions as in Fig. 3 are considered, in addition to the exchange correlation (XC) contribution.

5 Conclusion

We have described a linear scaling implementation of the trust-region self-consistent field (LS-TRSCF) method. In the LS-TRSCF method, each iteration consists of a crude optimization of the Roothaan-Hall energy giving a new density matrix (see Section 2.3) followed by the determination of an improved density matrix in the subspace containing the current and previous density matrices. A linear scaling algorithm is obtained using iterative methods to solve the level shifted Newton equations and sparse matrix algebra.

The convergence of the LS-TRSCF method is examined and for comparison the convergence of conventional SCF/DIIS calculations have been reported. The LS-TRSCF calculations show smooth and robust convergence and in several cases, the LS-TRSCF calculations converge where the SCF/DIIS calculations diverge. The convergence of the LS-TRSCF method is in general equally good for small and large systems. For small systems, a TRSCF implementation based on an explicit diagonalization of the Fock/KS matrix may be more efficient. However, for small systems the computational time for optimizing the density matrix is insignificant compared to the computational time for setting up the Fock/KS matrix. Consequently we recommend using the LS-TRSCF method for calculations on both small and large systems.

Acknowledgment

This work has been supported by the Danish Natural Research Council. We also acknowledge support from the Danish Center for Scientific Computing (DCSC).

References

[1] P. Pulay, *Chem. Phys. Lett.* **73** 393 (1980).

[2] C. A. White, B. G. Johnson, P. M. W. Gill and M. Head-Gordon, *Chem. Phys. Lett.* **230**, 8 (1994).

[3] C. A. White,B. G. Johnson, P. M. W. Gill and M. Head-Gordon, *Chem. Phys. Lett.* **253**, 268 (1996).

[4] M. C. Strain, G. E. Scuseria and M. J. Frisch, *Science* **271**, 51 (1996).

[5] M. Challacombe and E. Schwegler, *J. Chem. Phys.* **106**, 5526 (1997).

[6] Y. Shao, and M. Head-Gordon, *Chem. Phys. Lett.* **323**, 425 (2000).

[7] E. Schwegler and M. Challacombe , *J. Chem. Phys.* **105**, 2726 (1996).

[8] E. Schwegler, M. Challacombe and M. Head-Gordon , *J. Chem. Phys.* **106**, 9708 (1997).

[9] E. Schwegler and M. Challacombe , *J. Chem. Phys.* **111**, 6223 (1999).

[10] E. Schwegler and M. Challacombe , *Theor. Chem. Acc.* **104**, 344 (2000).

[11] C. Ochsenfeld, C. A. White and and M. Head-Gordon , *J. Chem. Phys.* **109**, 1663 (1998).

[12] J. C. Burant, G. E. Scuseria and M. J. Frisch, *J. Chem. Phys.* **105**, 8969 (1996).

[13] J. M. Pérez-Jordá and W. Yang, *Chem. Phys. Lett.* **241**, 469 (1995).

[14] B. G. Johnson, C. A. White, Q. Zang, B. Chen, R. L. Graham, P. M. W. Gill and M. Head-Gordon, in *Recent Developments in Density Functional Theory.* edited by J. M. Seminario (Elsevier Science, Amsterdam, 1996), Vol. 4

[15] R. E. Stratman, G. E. Scuseria and M. J. Frisch, *Chem. Phys. Lett.* **257**, 213 (1996).

[16] T. Helgaker, P. Jørgensen and J. Olsen. *Molecular Electronic-Structure Theory.* Wiley, New York, 2000.

[17] L. Thøgersen, J. Olsen, D. Yeager, P. Jørgensen, P. Sałek, T. Helgaker, *J. Chem. Phys.* **121** 16 (2004).

[18] L. Thøgersen, J. Olsen, A. Köhn, P. Jørgensen, P. Sałek, T. Helgaker, *J. Chem. Phys.* **123** 074103 (2005).

[19] R. McWeeny, *Rev. Mod. Phys.* **32**, 325 (1960).

[20] T. Helgaker, H. Larsen, J. Olsen and P. Jørgensen, *Chem. Phys. Lett.* **327**, 379 (2000).

[21] H. Larsen, J. Olsen and P. Jørgensen and T. Helgaker, *J. Chem. Phys.* **115**, 9685 (2001)

[22] Y. Shao, C. Saravanan, M. Head-Gordon and C. A. White, *J. Chem. Phys.* **118**, 6144 (2003).

[23] H. J. Aa. Jensen and P. Jørgensen, *J. Chem. Phys.* **80**, 1204 (1984).

[24] B. Lengsfield III, *J. Chem. Phys.* **73**, 382 (1980).

[25] R. Shepard, I. Shavitt and J. Simons, *J. Chem. Phys.* **76**, 543 (1982).

[26] P. Sałek *et al.*, *J. Chem. Phys.*, to be submitted.

[27] R. W. Nunes and D. Vanderbilt, *Phys. Rev. B* **50**, 17611 (1994).

[28] A. Schafer, H. Horn and R. Ahlrichs, *J. Chem. Phys.* **97**, 2571 (1992).